Journal of
Mechanical
Science and
Technology

Journal of Mechanical Science and Technology 21 (2007) 642~653

Optimal Design of Smart Panel Using Admittance Analysis

Lijie Zhao[a,b], Heung Soo Kim[a,*], Jaehwan Kim[a]

[a]*Creative Research Center for EAPap Actuator, Department of Mechanical Engineering, Inha University, 253 Yonghyun-Dong, Nam-Ku, Incheon, 402-751, Korea*

[b]*Department of Mechanical Engineering, Shenyang Institute of Aeronautical Engineering, 52 North Huanghe Street, Huanggu District, Shenyang, 110034, China*

(Manuscript Received May 2, 2006; Revised January 23, 2007; Accepted January 25, 2007)

Abstract

Optimal configuration of piezoelectric shunt structures is obtained by analyzing admittance of the system. The dissipated energy in the shunt circuit is a function of admittance. Therefore, admittance was selected as the cost function in the process of optimization. Taguchi method was used to determine the optimal configuration of piezoceramic patch bonded on the host structure. Full three dimensional finite element models were analyzed to simulate vibration modes of smart panel and to obtain the admittances of the system. Numerical admittance was validated by experiment. After optimizing process using admittance, the optimal configuration of piezoceramic patch was obtained. It is observed that the performance of smart panel can be predicted by analyzing admittance of piezoelectric structure and admittance can be used as a design index of smart panel.

Keywords: Smart panel; Structural vibration; Piezoelectric shunt; Admittance; Optimal design

1. Introduction

Recently, structural vibration or noise radiating from vibrating structures is a vital problem in the design of aircrafts, automobiles, ships and buildings. The study of smart structures in the past decade offers great potential in improving structural performance such as reducing vibration and acoustic emission (Chopra, 2002; Crawley, 1994; Kim and Lee, 2002). For conventional passive control, material properties or thickness of the structures have been addressed for the noise reduction (Belegunde et al., 1994; Pierre et al., 1995). The performance of passive control could be improved by the use of sound absorption materials attached on the main structure (Bolton et al., 1996), but it is impractical for low frequency bandwidth because of increasing amount of materials. Piezoelectric materials are employed as both actuators and sensors in the development of these structures by taking advantage of direct and converse piezoelectric effects. Since passive piezoelectric shunt system is simple, compact and low cost, piezoelectric shunt damping has been spotlighted in the field of vibration suppression (Hagood and Flotow, 1991; Law et al., 1996; Moheimani, 2003).

The piezoelectric shunt damping uses the principles of energy transfer and dissipation. Energy transfer from mechanical vibration into electrical energy is occurred in piezoceramic patches bonded on the structures. The transferred energy is dissipated by heat through resistor in shunt circuit networked to the structure (Law et al., 1996; Moheimani, 2003). Generally, piezoelectric shunt system consists of host plate, on which piezo ceramic patches are bonded, and electric shunt circuit networked to the piezo-

*Corresponding author. Tel.: +82 63 469 4723, Fax.: +82 63 469 4727
E-mail address: heungsookim@inha.ac.kr

electric structure, termed as smart panel. In order to dissipate external vibration or acoustical energy efficiently, piezoelectric structure must be constructed to generate more charges on the surface of piezoceramic patches bonded on the host structure, and shunt circuit must be tuned to dissipate the vibration energy at resonance into heat. Most researches have been concentrated on piezoelectric shunt circuit such as development of efficient shunt circuit, design of multi mode shunt circuit, and optimization of circuit parameters (Lesieutre, 1998; Kim et al., 2004; Behrens et al., 2001). Lately, several studies showed that the configuration of piezoceramic patches were important for designated target frequency and mode shape (Bianchini et al., 1997; Bianchini et al., 1998; Park et al., 2004). However, only mechanical characteristics of piezoelectric structures were considered. Based on these studies, it is difficult to design piezoelectric structure in real application and to predict the performance of piezoelectric shunt system. In order to overcome this, electro-mechanical characteristics of the piezoelectric structure need to be considered.

In this paper, admittance is introduced to represent electro-mechanical coupling of the piezoelectric structure. The relation between admittance and dissipated energy in shunt circuit is investigated first and then admittance is used as a performance index for optimal design of smart panel. Numerical admittance was obtained by finite element method. Taguchi method is used to obtain optimal configuration of smart panel. Admittance is used as a cost function in the optimal design process. Experiment was conducted to verify numerical admittance. Initial and optimal models of smart panel were tested for verifying the improvement of shunt performance.

2. Smart panel and admittance

Smart panel is configured as shown in Fig. 1. A piezoceramic patch is bonded on the surface of host structure and networked to the shunt circuit. Mechanical energy of vibration is transferred to electrical energy at the piezoceramic patch and the transferred electrical energy is dissipated at the shunt circuit.

2.1 Shunt damping

Piezoelectric system can be represented as an equivalent electric circuit as shown in Fig. 2 (Kim et al., 2000). Here, C_0 describes an inherent dielectric

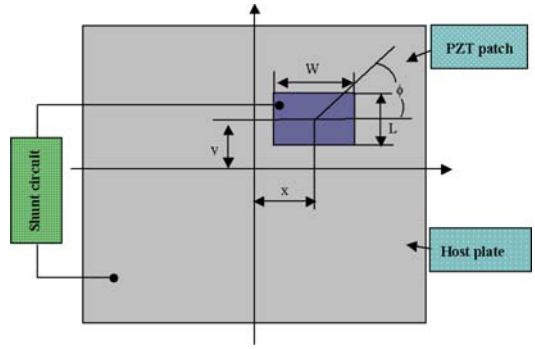

Fig. 1. Schematic view of piezoelectric patch on the host plate.

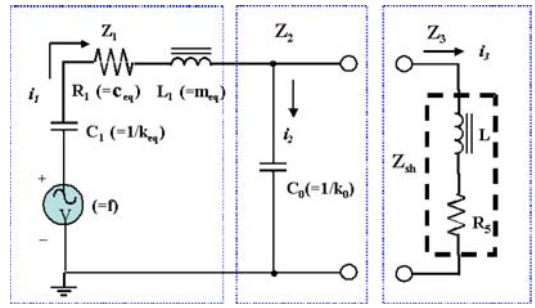

Fig. 2. Equivalent electrical circuit of piezoelectric smart structure.

capacity of piezoceramic patch (PZT: Lead Zirconate Titanate) which represents the compliance of piezoelectric patch ($1/k_0$), while L_1, R_1 , and C_1 imply mass (m_{eq}), damping (c_{eq}), and compliance ($1/k_{eq}$) of the structure, respectively (Kim and Kim, 2004). Piezoceramic patch, paralleled with a shunt circuit, has been used as a mechanical energy dissipation device. If a simple resistor is placed across the terminals of the piezoceramic patch, the piezoceramic patch acts only as a viscoelastic damper. If the network consists of a series inductor–resistor R–L circuit, the passive network combined with the inherent capacitance of the piezoceramic patch creates a damped electrical resonance. The resonance is tuned so that the piezoceramic patch acts as a tuned vibrational energy absorber (Hagood and Flotow, 1991).

2.2 Admittance and dissipated energy

Admittance analysis, that is the record of the spectrum of electrical admittance of the compound

resonator as a function of the exciting frequency, has changed the focus from the physical behavior of the system to its electrical opponents. The current resulting from the application of the voltage can be determined by the time derivative of the electric displacement, which in turn is related to the mechanical variables of the transducer (Mason, 1964). From knowledge of the current, the electrical behavior of the compound resonator under admittance analysis is derived. It should be addressed that the analysis is purely physical without use of any electrical analogues. Admittance can be measured at open circuit around the resonant frequency of the piezoceramic patch using impedance analyzer.

The smart panel on which the piezoceramic patch is bonded along with a shunt circuit can be modeled as shown in Fig. 2. The impedance at each branch of the equivalent circuit is described as follows (Kim and Kim, 2004).

$$Z_1(s) = m_{eq}s + \frac{k_{eq}}{s} + c_{eq} = j\omega L_1 + \frac{1}{j\omega C_1} + R_1 \tag{1}$$

$$Z_2(s) = \frac{k_0}{s} = \frac{1}{j\omega C_0} \tag{2}$$

$$Z_3(s) = j\omega L + R \tag{3}$$

where,

Z_1 : impedance of the host structure

Z_2 : impedance of the piezoceramic patch

Z_3 : impedance of the shunt circuit

Because the total impedance of the system can be calculated as

$$Z = Z_1 + \frac{Z_2 Z_3}{Z_2 + Z_3} \tag{4}$$

The admittance of the piezoelectric patch is the reciprocal of its impedance as follows.

$$|Y| = \frac{1}{|Z|} \tag{5}$$

One can define the induced power in terms of the equivalent electrical circuit according to Fig. 2. The induced power of the system under external excitation is

$$P_{in} = \frac{1}{2}\left|V \cdot i_1^*\right| = \frac{1}{2}\left|\frac{i}{Y} \cdot i_1^*\right| = \frac{1}{2}\left|\frac{1}{Y}\right| \cdot |i_1|^2 \tag{6}$$

where i_1^* is the complex conjugate of the current i_1.

In open circuit state, i.e. $Z_3 = \infty$, total current of piezoceramic patch generated under external excitation, i_O, is given as follows.

$$i_O = \frac{V_O}{(Z_1 + Z_2)} = V_O \cdot Y_{12} \tag{7}$$

where, $Y_{12} = (Z_1 + Z_2)^{-1}$ represents admittance of piezoelectric structure in open circuit. The voltage, V_O represents voltage of piezoelectric patch in open circuit. When shunt circuit is connected to the structure, i,e. $Z_3 \neq \infty \neq 0$, the total current of piezoelectric shunt system can be expressed as follows.

$$i_1 = i_2 + i_3 = V_3 \cdot \left(\frac{Z_2 + Z_3}{Z_2 \cdot Z_3}\right) \tag{8}$$

If same external excitation is applied to the smart panel before and after connecting shunt circuit, total current generated in each system is the same and can be expressed as $i_O = i_1$. From Eqs. (7) and (8), voltage applied to shunt circuit, V_3, and current flowing in the shunt circuit, i_3, are expressed as follows.

$$V_3 = V_O \cdot Y_{12} \cdot \frac{Z_2 \cdot Z_3}{Z_2 + Z_3} \tag{9}$$

$$i_3 = \frac{Z_2}{Z_2 + Z_3} \cdot i_O \tag{10}$$

Meanwhile, the dissipated power can be described as

$$\begin{aligned} P_D &= \frac{1}{2}\left|V_2 \cdot i_3^*\right| = \frac{1}{2}\left|(\mathrm{Re}(Z_3) \cdot i_3) \cdot i_3^*\right| = \frac{1}{2}\mathrm{Re}(Z_3) \cdot |i_3|^2 \\ &= \frac{1}{2}\mathrm{Re}(Z_3) \cdot \left|\frac{Z_2}{Z_2 + Z_3}\right|^2 \cdot |i_O|^2 \\ &= \frac{1}{2}\mathrm{Re}(Z_3) \cdot \left|\frac{Z_2}{Z_2 + Z_3}\right|^2 \cdot |V_O|^2 \cdot |Y_{12}|^2 \end{aligned} \tag{11}$$

From Eq. (11), the dissipated power is proportional to the quadratic form of electro-mechanical characteristic values ($|Y_{12}|^2$) of piezoelectric structure in open circuit. If the voltage V_O is applied to the system, admittance is a single independent constant. On the other hand, the dissipated power is only a function of admittance of piezoelectric structure in open circuit. Therefore, the reduction of vibration in

the piezoelectric shunt system is dependent on admittance of piezoelectric structure and admittance can be regarded as a performance index in designing smart panel.

2.3 Formulation of admittance

Finite element analysis is an effective method for analysis of structural response, because it is applicable to arbitrarily shapes, geometries and boundaries. Admittance of piezoelectric structure is analyzed by Electro-Mechanical Impedance (EMI) model (Liang, Sun and Rogers, 1996) or the finite element method (Powell et al., 1998; Kim et al., 1996; Varadan et al., 1996). Admittance is consisted of real part, conductance and imaginary part, susceptance. The magnitude of electro-mechanical coupling is represented by conductance. After finite element discretizing, equations of motion for the piezoelectric structure in matrix form are expressed as follows (ANSYS INC. 1999).

$$\begin{Bmatrix} [M] & [0] \\ [0] & [0] \end{Bmatrix} \begin{Bmatrix} [\ddot{u}] \\ [\ddot{\phi}] \end{Bmatrix} + \begin{Bmatrix} [D] & [0] \\ [0] & [0] \end{Bmatrix} \begin{Bmatrix} [\dot{u}] \\ [\dot{\phi}] \end{Bmatrix} + \begin{Bmatrix} [K] & [K_{u\phi}] \\ [K_{u\phi}]^t & [K_{\phi}] \end{Bmatrix} \begin{Bmatrix} [u] \\ [\phi] \end{Bmatrix} = \begin{Bmatrix} [F] \\ [Q] \end{Bmatrix} \tag{12}$$

$$|Y| = \left| \frac{i}{V} \right|, \quad i = j\omega \sum_i Q_i \tag{13}$$

$$Y = G + jB \tag{14}$$

where,

- $[F]$, $[u]$: vector of nodal structural forces and displacements
- $[M]$, $[D]$, $[K]$: structural mass, damping and stiffness matrix
- $[Q]$, $[\phi]$: vector of nodal electrical charges and potential
- $[K_{u\phi}]$, $[K_{\phi}]$: piezoelectric coupling and dielectric conductivity matrix
- "t" : transposed
- i, V : current and voltage
- Y, G, B : admittance, conductance and susceptance
- Q_i : the point charge of the i-th node on on the electrode

To formulate above equation, commercial finite element code, ANSYS, was used. From the above equations, mode shapes and natural frequencies of smart panel were extracted through modal analysis and admittances of piezoceramic patch were obtained through harmonic analysis.

3. Optimization using taguchi method

Robust Design Method, called Taguchi method, is executed in this study. It differentiates traditional approach which would be to design experiments that identified all possible combination for a given set of variables. It is termed as full factorial design and takes into account a large number of trials, which is costly and time consuming. Taguchi method considers not only the average of data but also the variance of data in its process. In robust design, the signal constituent S and the noise constituent N are extracted from signal to noise ratio (SN rate). The SN ratio shows the robustness of the characteristic value in the function.

Two considerations are focused in Taguchi method. The first, orthogonal arrays, which are employed for many experimental situations, are introduced from the viewpoint of the pragmatist who is always trying to make product or process improvement decisions with the minimum amount of test data. The second, a standard analyzing method which analysis of variance (ANOVA) is applied to the orthogonal array type of trials. This technique does not directly analyze the data, but rather determine the variability (variance) of the data (Ross, 1996; Roy, 1990). Through it, which factor has more influence and which one has less are determined. The result of calculation indicates how to combine different factors in their proper settings to get the best result. The advantage of this approach is that it can replace full factorial design using partially factorial design. The results can be tabulated and shown graphically simultaneously (Ross, 1996). The flow chart of Taguchi method is shown in Fig. 3. Additionally, the combination of standard experimentation design techniques and analysis method in Taguchi approach produces consistency and reproducibility.

In Taguchi method, static analysis and dynamic analysis are embedded. The signal to noise ratio (S/N ratio) is used to measure the sensitivity of the quality characteristic being investigated in a controlled manner. Taguchi has created a transformation of the repetition data to another value which is a measure of the variation present. The transformation is defined as S/N ratio. The results of S/N ratio are used to compute the main effects of the individual factors and

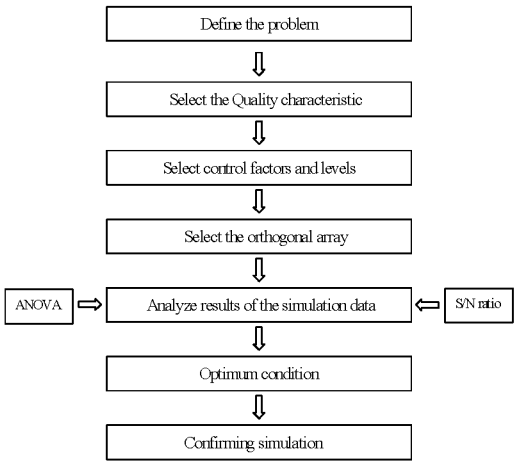

Fig. 3. Flow chart of Taguchi method.

Table 1. Control factors of smart panel.

Factors		Levels		
		1	2	3
ϕ	Rotational angle (°)	0	45	
x	x coordinate (mm)	0	25	50
y	y coordinate (mm)	0	25	50
L	Length (mm)	50	75	100
W	Width (mm)	50	75	100

it is usually calculated by the equation:

$$S/N = -10\log(MSD) \tag{15}$$

where MSD represents the mean squared deviation of the set. In addition to the S/N ratio, the main effect can also be plotted for a visual inspection of the parameters' effects (Roy, 1990; Ramberg et al., 1991).

4. Numerical results

A square aluminum plate with surface-bonded piezoceramic patch was considered as shown in Fig. 1. The performance of piezoelectric shunt depends on location, size and shape of piezoceramic patch. In the present study, the suppression of radiation mode of smart panel is pursued for the reduction of sound transmission of panel. Therefore, the location (X and Y coordinates), size (width W and length L), and rotational angle of piezoceramic patch on the host plate were defined as the design parameters in the present study. The size of the aluminum plate is 350 mm×350 mm×1.5 mm. A piezoceramic patch, classified as PZT-5H, was selected as the shunt damping material and bonded on the surface of the aluminum plate. The material properties are shown in Appendix. The size of piezoceramic patch is restricted from 50 mm to 100 mm for actual implementation. The location of piezoceramic patch is considered to cover major area of aluminum host plate. One representative rotational shape of piezoceramic patch is investigated in the present study. The size and location are assumed to have three levels. Therefore, control factors for optimal configuration of smart panel can be defined as shown in Table 1. The thickness of piezoceramic patches is all 0.5 mm.

Table 2. Orthogonal array table of L_{18}.

Trial No.	Column No.				
	1	2	3	4	5
1	1	1	1	1	1
2	1	2	2	2	2
3	1	3	3	3	3
4	1	2	1	1	2
5	1	2	2	2	2
6	1	2	3	3	1
7	1	3	1	2	1
8	1	3	2	1	2
9	1	3	3	1	3
10	2	1	1	3	3
11	2	1	2	1	1
12	2	1	3	2	2
13	2	2	1	2	3
14	2	2	2	3	1
15	2	2	3	1	2
16	2	3	1	3	2
17	2	3	2	1	3
18	2	3	3	2	1

4.1 Numerical analysis using taguchi method

Taguchi method is used to find partial configurations from full configurations according to the parameters as well as levels. Since 'L_n orthogonal array' in Taguchi optimization implies n tentative models can be extracted from combinations of full parameters. The 'n' value in 'L_n' is dependant on the control factors and their levels. Therefore, referring to Table 1, the L_{18} orthogonal array is used as shown in Table 2. The parameters and their combinations of which Taguchi method made use were selected from Tables 1 and 2. It is noted that the trial number in Table 2 refers to partial configuration of piezoelectric patch on the host structure instead of full combinations. In virtue of orthogonal array in Table 2, the

Table 3. Resonances and admittances of numerical models.

No.	Frequency(Hz)	Conductance(1/Ω)	Admittance(1/Ω)	Charge (C)
1	135.10	3.97016E-5	1.16863E-4	1.3774E-7
	515.67	0.00104	0.00121	3.7364E-7
2	132.34	1.74104E-4	3.08259E-4	3.7091E-7
	285.26	7.47683E-5	5.22005E-4	2.9141E-7
	516.98	0.00347	0.00373	1.1489E-6
3	130.95	3.09123E-4	5.18967E-4	6.3107E-7
	281.99	0.00151	0.00178	8.5377E-7
	528.43	0.00257	0.0033	9.9441E-7
4	134.01	6.3413E-05	8.8550E-05	1.0522E-07
	280.69	1.1791E-05	1.4546E-04	8.2522E-08
	518.34	1.0255E-03	1.0540E-03	3.2379E-07
5	131.57	9.6060E-05	2.3475E-04	2.8411E-07
	283.24	1.0973E-04	4.5865E-04	2.5785E-07
	436.16	9.0857E-05	4.6223E-04	1.6875E-07
	525.63	6.4541E-04	1.4151E-03	4.2868E-07
6	135.89	5.2862E-05	1.1174E-04	1.3094E-07
	284.28	3.9891E-04	4.1678E-04	2.3346E-07
	424.75	9.5573E-05	3.5383E-04	1.3265E-07
	513.62	9.9283E-05	3.9730E-04	1.2317E-07
7	132.05	1.7213E-05	5.1055E-05	6.1566E-08
	282.30	5.0692E-05	5.6150E-05	3.1672E-08
	526.60	8.2138E-05	2.7234E-04	8.2352E-08
8	132.51	1.2046E-04	2.0050E-04	2.4093E-07
	280.36	7.4864E-04	8.9316E-04	5.0729E-07
	432.48	1.2459E-04	2.0170E-04	7.4265E-08
	527.12	7.2054E-04	8.7423E-04	2.6409E-07
9	135.55	3.5366E-05	7.4414E-05	8.7417E-08
	284.21	1.7203E-04	4.1200E-04	2.3083E-07
	425.06	4.6366E-04	4.6439E-04	1.7397E-07
	512.35	2.3163E-05	2.7043E-04	8.4049E-08
10	123.22	3.6975E-04	3.8093E-04	4.9227E-07
	500.83	5.8481E-03	6.1750E-03	1.96331E-06
11	133.63	2.6739E-05	4.3990E-05	5.2419E-08
	281.91	1.8647E-05	1.0636E-04	6.0079E-08
	511.47	5.1965E-04	5.2224E-04	1.62588E-07
12	131.30	7.3509E-05	9.4047E-05	1.14057E-07
	280.55	2.5133E-04	2.5378E-04	1.44043E-07
	517.71	9.9389E-04	1.0292E-03	3.16567E-07
13	128.70	1.6630E-04	2.5995E-04	3.21621E-07
	279.27	1.2840E-04	1.9462E-04	1.10968E-07
	509.69	2.1344E-03	2.2518E-03	7.0349E-07
14	134.6	7.4659E-05	9.1322E-05	1.08036E-07
	277.15	1.9020E-04	2.1265E-04	1.22175E-07
	420.56	6.7289E-05	2.7057E-04	1.02446E-07
	508.31	2.6644E-04	2.8127E-04	8.81111E-08
15	133.95	1.6498E-05	6.0527E-05	7.19524E-08
	278.75	1.1343E-04	1.5613E-04	8.91883E-08
	426.37	2.5148E-05	2.0720E-04	7.73809E-08
	511.46	7.2633E-05	2.4513E-04	7.63189E-08
16	129.80	6.0859E-05	1.3704E-04	1.68116E-07
	280.79	2.4528E-04	2.6671E-04	1.5125E-07
	516.90	6.2765E-04	6.6643E-04	2.05298E-07
17	134.01	4.6218E-05	1.1011E-04	1.3084E-07
	278.48	2.4944E-04	2.4946E-04	1.42641E-07
	418.78	1.5999E-04	3.4098E-04	1.29651E-07
	503.83	1.3680E-03	3.7577E-04	1.18764E-07
18	134.69	8.0407E-06	6.0612E-05	7.16577E-08
	276.50	5.1525E-05	7.1410E-05	4.11251E-08
	422.11	7.3304E-05	1.0963E-04	4.13563E-08
	515.50	1.0940E-05	2.0954E-04	6.4725E-08

full factorial design was reduced from $3^4 \times 2^1 = 162$ trials to 18 trials. The 18 finite element models were analyzed by ANSYS to obtain strong radiation modes and admittances at resonances for optimizing process.

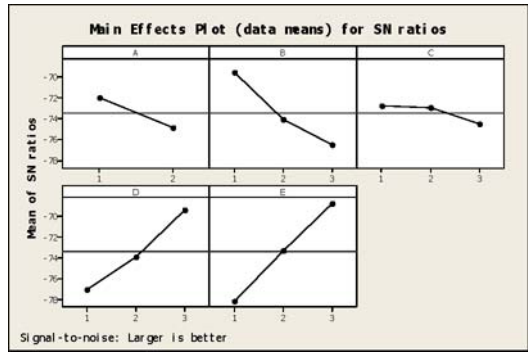

Fig. 4. Main effects plots for S/N ratio.

4.2 Modal and harmonic analyses

In terms of FEM code, modal and harmonic analyses were conducted to obtain the mode shapes of the structure and the admittances at different resonant frequencies, respectively. Element type of solid 5 in ANSYS is used to discretize piezoceramic patch and solid 45 for aluminum plate. Eighteen models obtained from Sec. n 4.1 are discretized and analyzed using modal and harmonic solvers in ANSYS. Natural frequencies were extracted by modal analysis. The admittances and charge values at different resonant frequencies were obtained by harmonic analysis. Accordingly, the admittances and natural frequencies at strong radiation modes were obtained form admittance and mode shapes of piezoelectric structure as shown in Table 3.

4.3 Optimization using taguchi method

In the present study, the DOE (Design of Experiments) module in Minitab is used for Taguchi optimization (Ryan and Joiner, 1994). The admittances derived from ANSYS according to the 18 models were regarded as performance index and put into the required table of Taguchi method. Static analysis was conducted in this study. An optimal configuration of the patch on host structure was derived from 18 models. In this paper, the objective value (signal to noise ratio: S/N) of cost function (admittance) is set to be the-Larger-the-Better, which is defined as Eq. (15). In which MSD = l/n Σ (l/y) is the mean square deviation, y is the extracted admittances at strong radiation modes from 18 tentative models determined by orthogonal array (Tables 2 and 3), and n is the number of model. The Larger-the-Better means that MSD is minimized. Minimizing the MSD represents maximizing the S/N.

Table 4. Response and main effects for S/N ratio.

Level	A	B	C	D	E
1	71.99	69.60	72.76	77.01	78.13
2	74.86	74.12	72.96	73.89	73.34
3		76.55	74.56	69.38	68.80
Delta	2.86	6.94	1.80	7.63	9.34
Rank	4	3	5	2	1

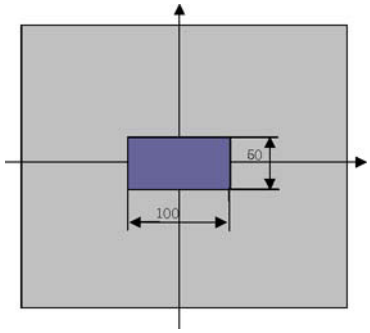

(a) Initial configuration

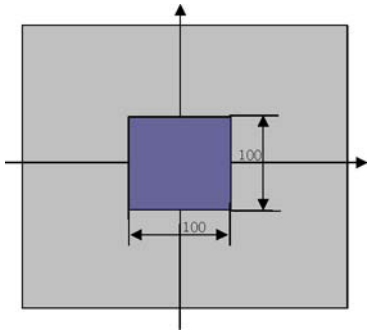

(b) Optimal configuration

Fig. 5. The initial and optimal configuration of smart panel.

As result, one can obtain S/N ratio for each model by use of the admittances at different strong radiation modes. The results of optimization process are shown in the main effect plot (Fig. 4) and S/N values (Table 4). According to the function of 'the-Larger-the-Better', the optimal configuration is (1 1 1 3 3) case, which represents that the piezoceramic patch is located at the center of the host structure and the size is 100 mm×100 mm, the rotational angle of piezo-electric patch is 0°.

4.4 Analysis of initial model and optimal model

In order to correlate the design numerically and experimentally, two models, the initial and optimal configurations of smart panel, were selected in this paper. The initial configuration of piezoceramic patch is 100 mm×50 mm×0.5 mm and the patch is located

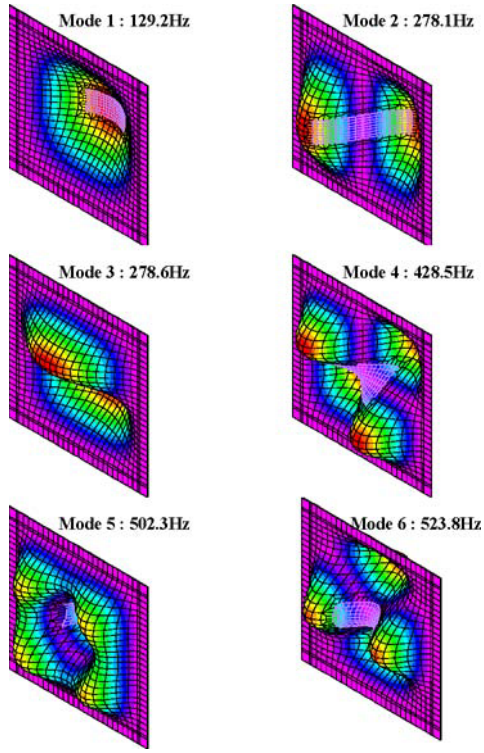

Fig. 6. Mode shapes and natural frequencies of initial model.

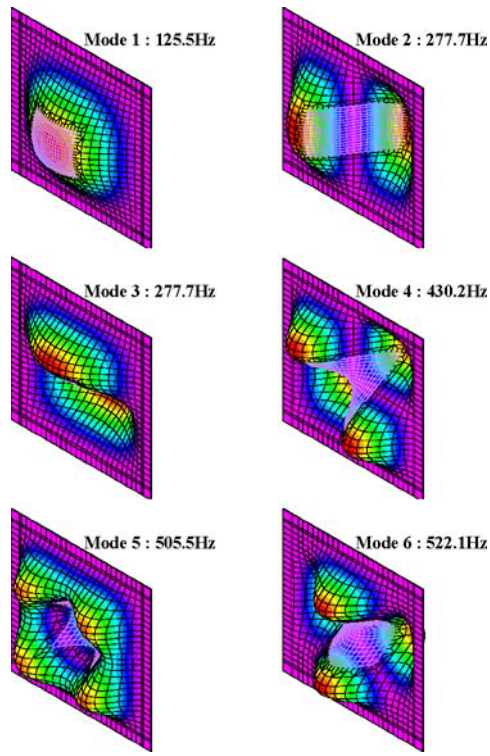

Fig. 7. Mode shapes and natural frequencies of optimal model.

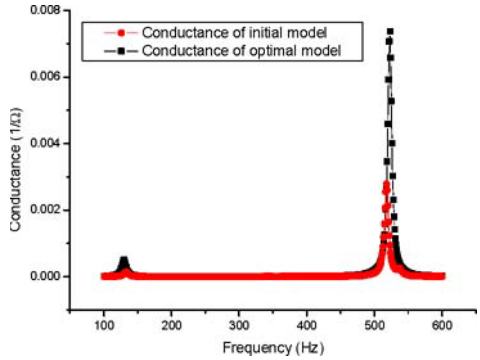

Fig. 8. Conductances of initial and optimal model.

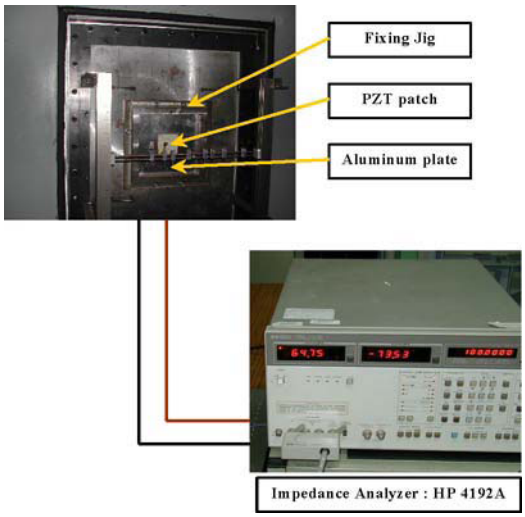

Fig. 9. Experimental apparatus for admittance analysis.

at the center of aluminum plate [Fig. 5(a)]. The optimal configuration of piezoceramic patch obtained by Taguchi method is 100 mm×100 mm×0.5 mm and also located at the center of aluminum plate [Fig. 5(b)]. Using finite element code, the modal analysis was performed first. The mode shapes and natural frequencies were extracted as shown in Figs. 6 and 7. Then, the numerical admittances were obtained by harmonic analysis for two models. The comparison is presented in Fig. 8. It is clearly observed that the conductance of optimal model is larger than that of initial model under same external excitation.

5. Experimental results

Numerical admittance and shunt performance were validated by two experiments.

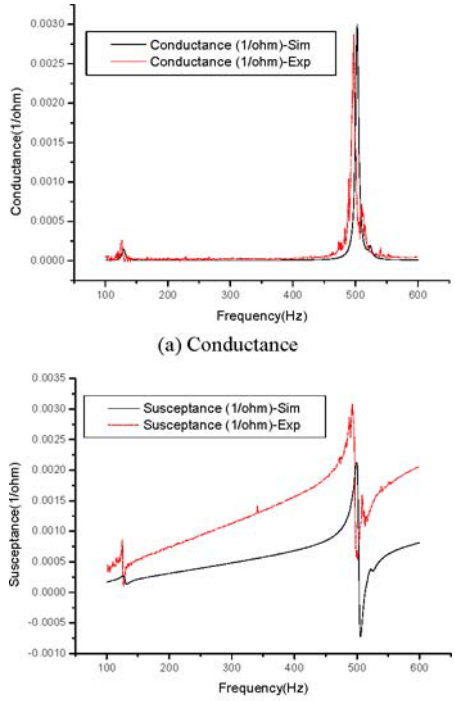

Fig. 10. Comparison of experimental and numerical admittance of initial model.

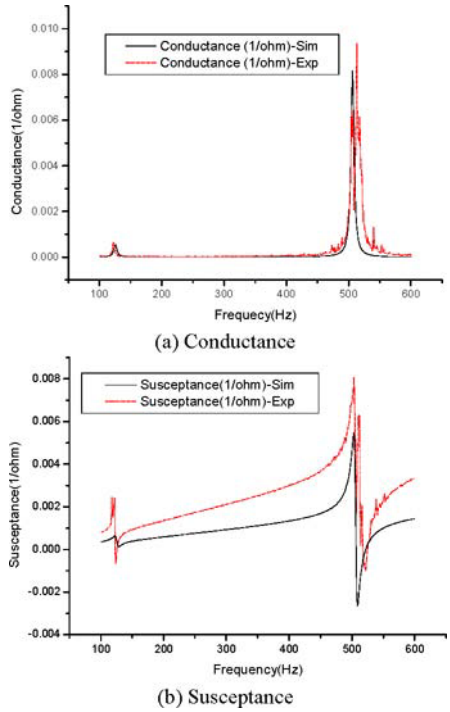

Fig. 11. Comparison of experimental and numerical admittance of optimal model.

Table 5. Comparisons of natural frequencies for initial and optimal model.

Model	FEM	Experiment	Comparison
	Frequency (Hz)	Frequency (Hz)	
100mmX50mm	129	125	3.1%
	502	496	1.2%
100mmX100mm	126	122	2.4%
	506	512	1.4%

5.1 Admittance test

The admittances for initial and optimal model were measured by using the impedance analyzer (HP4192 A). The experimental setup is presented in Fig. 9. The admittances were measured at open circuit state. According to the poling direction, the positive electrode of the impedance analyzer was connected with the top surface of the piezoelectric patch that was away from host plate. The negative electrode of the impedance analyzer was connected with the host plate. Comparisons between experimental and numerical admittances of initial and optimal model are presented in Figs. 10 and 11. Two peaks of conductance and susceptance represent first and fifth natural frequencies of square plate, which are strong radiation mode. The comparisons of natural frequencies are listed in Table 5. The natural frequencies obtained by experiments are shifted down 3.1% and 1.2% for initial configuration, 2.4% and 1.4% for optimal configuration, respectively. As result, it is observed that the conductances (the real part of admittances) and natural frequencies correlate well between numerical and experimental results.

5.2 Shunt damping test

For the sake of testing the performance of vibration reduction of smart panel, an actuating piezoceramic patch is bonded on the center of the aluminum plate, where is the opposite side of aluminum plate for shunting piezoceramic patch. The size of piezoceramic patch for exciting panel is 50 mm×50 mm×0.5 mm. Experimental setups for piezoelectric shunt damping are presented in Fig. 12. An accelerometer (Charge Accelerometer Type 4374, B&K) was attached on the surface of the piezoceramic patch to measure time and frequency response of smart panel. Resonant shunt circuit was connected to the piezoceramic patch. The performance of shunt damping was processed by PORTABLE FFT ANALYZER CF-3200 manufactured by ONO SAKK company. Figures 13 and 14 present frequency responses of vibration through optimally tuning two target modes with and without piezoelectric shunt damping for initial model and optimal model, respectively. Comparison of shunt performance is listed in Table 6. In initial model configuration, the vibrations are suppressed 16 dB at

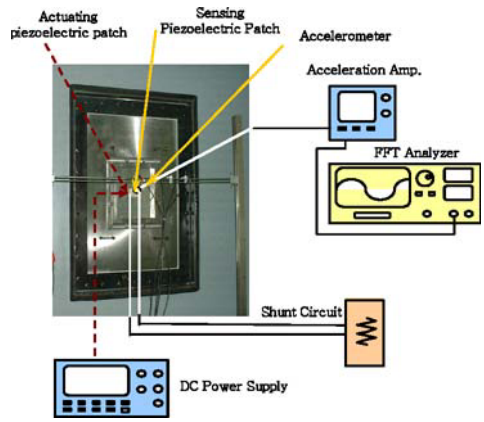

Fig. 12. Experimental setup for piezoelectric shunt damping.

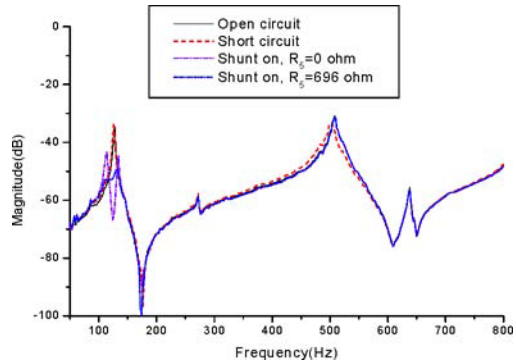

(a) First mode

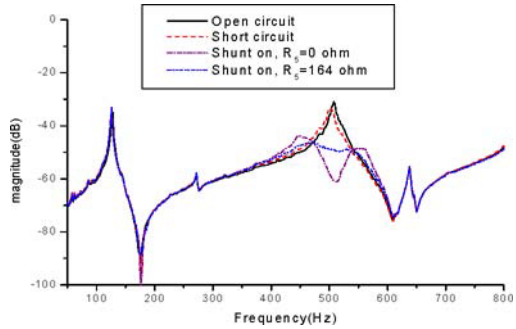

(b) Fifth mode

Fig. 13. FRF responses of initial configuration.

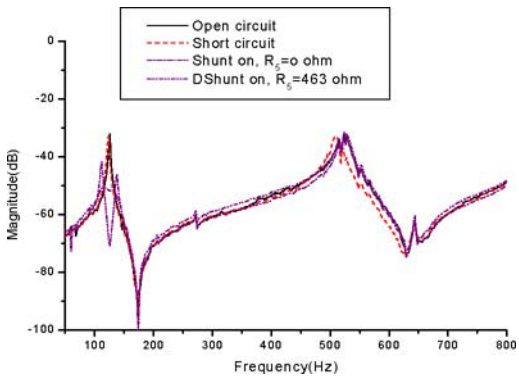

(a) First mode

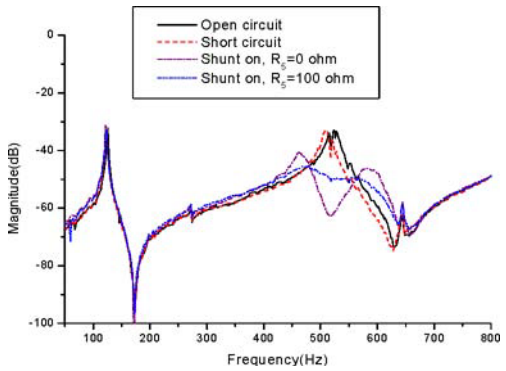

Fig. 14. FRF responses of optimal configuration.

Table 6. Comparisons of the piezoelectric shunt performance between initial and optimal model.

Mode Number	Initial Model		Optimal Model		Improvement
1	125 Hz	-16 dB	122 Hz	-20 dB	25 %
5	496 Hz	-18 dB	512 Hz	-22 dB	22 %

first mode while 18 dB at fifth mode. In optimal model configuration, the magnitudes of vibration are reduced to 20 dB at first mode while 22 dB at fifth mode. It is illustrated that the performance of piezoelectric shunt is improved by 25% at first mode and 22% at fifth mode from the initial model to optimal model. From the observation, optimal configuration of piezoelectric shunt structure can be obtained using admittance as a design parameter.

6. Conculsion

In this study, optimal configuration of smart panel was obtained using admittance. Admittance of piezoelectric system was introduced to represent electromechanical coupling of smart panel. The dissipated power of smart panel was only a function of admittance of piezoelectric patch in open circuit. Therefore, admittance was selected as the performance index for optimal design of smart panel. Piezoceramic patch bonded on the host structure was configured by size, location, as well as rotational angle on the host plate. Control parameters were selected to suppress radiating mode of smart panel for the reduction of sound transmission. Each parameter owned three levels except the rotational angle owning two levels in the process of optimal design. Taguchi method was used to obtain the optimal configuration of piezoceramic patch bonded on the smart panel. Initial and optimal models were investigated to correlate numerical and experimental results. Two experiments were conducted to validate the result of optimal design. Numerical and experimental admittances provided good correlations. In terms of shunt damping test, the performance of piezoelectric shunt damping was improved by 25% at first mode and 22% at fifth mode by comparing the optimal configuration with the initial configuration. It is concluded that the performance of smart panel can be predicted by analyzing admittance of piezoelectric structure and admittance can be used as a design index of smart panel.

Appendix

Aluminum plate:Young's modulus=70 GPa, Possion's ratio=0.345, Density=2698(kg/m^3).

PZT-5H: Density=7500 kg/ m^3,

Elastic property matrix with constant electric field is

$$\begin{bmatrix} 12.6 & 7.95 & 8.41 & 0 & 0 & 0 \\ & 12.6 & 8.41 & 0 & 0 & 0 \\ & & 11.7 & 0 & 0 & 0 \\ & & & 2.35 & 0 & 0 \\ & Sym & & & 2.3 & 0 \\ & & & & & 2.3 \end{bmatrix} \times 10^{10}(N/m^2)$$

Piezoelectric strain matrix

$$\begin{bmatrix} 0 & 0 & 0 & 0 & 0 & 17 \\ 0 & 0 & 0 & 0 & 17 & 0 \\ -6.55 & -6.55 & 23.3 & 0 & 0 & 0 \end{bmatrix}^T \times F/m^2$$

Dielectric property matrix with constant strain is

$$\begin{bmatrix} 1700 & 0 & 0 \\ 0 & 1700 & 0 \\ 0 & 0 & 1470 \end{bmatrix} (C/m^2)$$

Acknowlegement

This work was supported by the Creative Research Initiatives Program of Korea Science and Engineering Foundation (KOSEF).

References

ANSYS INC., 1999, ANSYS Theory Manual Ver. 5.5. SAS IP.

Behrens, S., Fleming, A. J., Moheimani, S. O. R., 2001, "New Method for Multiple-Mode Shunt Damping of Structural Vibration Using Single Piezoelectric Transducer," *Proceedings of SPIE 2001*, Vol. 4331, pp. 239~250.

Belegunde, A. D., Salagame, R. R., Koopmann, G. H., "A General Optimization Strategy for Sound Power Minimization," *Structural Optimization*, No. 8, 1994, pp. 113~119.

Bianchini, E., Spangler, R., 1998, "The Use of Piezoelectric Devices to Control Snowboard Vibrations," *Proceeding of SPIE Conference on Integrated Systems*, Vol. 3329, pp. 106~114.

Bianchini, E., Spangler, R., Pandell, T., 1997, "The Use of Piezoelectric Dampers for Improving the Fell of Golf Clubs," *Proceedings of SPIE Conference on Smart Structures and Integrated Systems*, Vol. 3688, pp. 824~834.

Bolton, J. S., Shiau, N. M., Kang, Y. J., "Sound Transmission Through Multi-Panel Structures Lined with Elastic Porous Materials," *Journal of Sound and Vibration*, Vol. 191, No. 3, 1996, pp. 317~347.

Chopra, I., 2002, "Review of State-of-Art of Smart Structures and Integrated Systems," *AIAA Journal*, Vol. 40, No, 11, pp. 2145~2187.

Crawley, E. F., 1994, "Intelligent Structures for Aerospace: A Technology Overview and Assessment," *AIAA Journal*, Vol. 32, No. 8, pp. 1689~1699.

Hagood, N. W., Flotow, A. V., 1991, "Damping of Structural Vibrations with Piezoelectric Material and Passive Electrical Networks," *Journal of Sound and Vibration*, 146, No. 2, pp. 243~268.

Kim, J., Kim, J. H., 2004, "Multimode Shunt Damping of Piezoelectric Smart Panel for Noise Reduction," *Journal of Acoustic Society America*, Vol. 116, No. 22, pp. 942~948.

Kim, J., Lee, J. K., 2002, "Broadband Transmission Noise Reduction of Smart panels Featuring Piezoelectric Shunt Circuits and Sound Absorbing Material," *Journal of Acoustic Society America*, Vol. 112, No. 3, pp. 990~998.

Kim, J., Ryu,Y. H., Choi, S. B., 2000, "New Shunting Parameter Tuning Method for Piezoelectric Damping Based on Measured Electrical Impedance," *Smart Materials and Structures*, Vol.9, No. 6, pp. 868~877.

Kim, J., Varadan, V. V., Varadan, V. K., Bao, X. Q., 1996, "Finite-Element Modeling of a Smart Cantilever Plate and Comparison with Experiments," Smart Materials and Structures, Vol. 5, No. 12, pp. 165~170.

Law, H. H., Rossiter, P. L., Simon, G. P., Koss, L. L., 1996, "Characterization of Mechanical Vibration Damping by Piezoelectric Materials," *Journal of Sound and Vibration*, Vol. 197, No. 4, pp. 489~513.

Lesieutre, G. A., 1998, "Vibration Damping and Control Using Shunted Piezoelectric Materials," *The Shock and Vibration Digest*, Vol. 30, No. 3, pp. 187~195.

Liang, C., Sun, F. P., Rogers, C. A., 1996, "Electromechanical Impedance Modeling of Active Material Systems.," *Smart Materials and Structures*, Vol. 5, No. 11, pp. 171~186.

Mason, W. P., 1964, Physical Acoustics, Principles and Methods Vol. I - Part A, New York: Academic Press.

Moheimani, S. O. R., 2003, "A Survey of Recent Innovations in Vibration Damping and Control Using Shunted Piezoelectric Transducers," *IEEE Transactions on Control Systems Technology*, Vol. 11, No. 4, pp. 482~494.

Park, J. S., Lim, S. C., Choi, S. B., Kim, J. H., Park, Y. P., 2004, "Vibration Reduction of a CD-ROM Drive Base Using a Piezoelectric Shunt Circuit," *Journal of Sound and Vibration*, Vol. 269, No. 3, pp. 1111~1118.

Pierre, R. L. St. Jr., Koopmann, G. H., "A Design Method for Minimizing the Sound Power Radiated from Plates by Adding Optimally Sized, Discrete Masses," *Transaction of the ASME* Vol. 117, 1995, pp. 243~151.

Powell, D. J., Mould, J., Wojcik, G. L., 1998, "Dielectric and Mechanical Absorption Mechanisms for Time Frequency Domain Transducer Modeling," *IEEE Ultrasonic Symposium Proceedings*, Vol. 2, pp. 1019~

1024.

Ramberg, J. S., Sanchez, S. M., Sanchez, P. J., Hollick, L. J., 1991, "Designing Simulation Experiments: Taguchi Methods and Response Surface Metamodels," *Proceedings of the 1991 Winter Simulation Conference*, ed. B.L. Nelson, W.D. Kelton, and G.M. Clark, 167~176. WSC Board of Directors.

Ross, P. J., 1996, Taguchi Techniques for Quality Engineering, Second Edition. The Mcgraw-Hill Companies, Inc.

Roy, R., 1990, A Primer on the Taguchi Method. New York: Van Nostrand Reinhold.

Ryan, B. F., Joiner, B. L., 1994, Minitab Handbook, Belmont, Calif: Duxbury Press.

Varadan, V. V., Lim, Y. H., Varadan, V. K., 1996, "Closed Loop Finite-Element Modeling of Active/ Passive Damping in Structural Vibration Control," *Smart Materials and Structures*, Vol. 5, No. 9, pp. 685~694.